Dalton Transactions

ROYAL SOCIETY OF CHEMISTRY

PAPER

View Article Online
View Journal | View Issue

Cite this: *Dalton Trans.*, 2022, **51**, 11776

Trinuclear zinc calix[4]arenes: synthesis, structure, and ring opening polymerization studies†

Tian Xing,[a] Josef W. A. Frese,[b] Max Derbyshire,[b] Mollie A. Glenister,[b] Mark R. J. Elsegood [b] and Carl Redshaw [*a]

The trinuclear zinc calix[4]arene complexes $[Zn_3(O_2CCH_3)_2(L(O)_2(OMe)_2)_2{\cdot}x$MeCN ($x$ = 7.5, **1**; x = 6, **1′**), $[Zn_3(O_2CCH_3)_2(L(O)_2(O$*n*$Pr)_2)_2{\cdot}5$MeCN (**2**·5MeCN), $[Zn_3(OEt)_2(L(O)_2(OMe)_2)_2]{\cdot}4$MeCN (**3**·4MeCN), $[Zn_3(OEt)_2(L(O$pentyl$)_2)_2]{\cdot}4.5$MeCN (**4**·4.5MeCN) and $[Zn_3(OH)_2(L(O)_2(O$*n*-pentyl$)_2]{\cdot}8$MeCN (**5**·8MeCN) have been isolated from reaction of $[(ZnEt)_2(L(O)_2(OR)_2)_2]$ ($L(OH)_2(OR)_2$ = 1,3-dialkoxy-4-*tert*-butylcalix[4]arene; R = methyl, *n*-propyl or pentyl) and the reagents acetic acid, ethanol, and presumed adventitious water, respectively. Attempts to make **5** *via* a controlled hydrolysis led only to the isolation of polymorphs of $(L(OH)_2(O$pentyl$)_2{\cdot}$MeCN. Reaction of $[Zn(C_6F_5)_2]$ with $L(OH)_2(O$pentyl$)_2$, in the presence of K_2CO_3, led to the isolation of the complex $[Zn_6(L(O$*n*-pentyl$))_2(OH)_3(C_6F_5)_3(NCMe)_3]{\cdot}3$MeCN (**6**·3MeCN). The molecular structures of **1–6** reveal they all contain a near linear (163 to 179°) Zn_3 motif. In **1–5**, a central tetrahedral Zn centre is flanked by trigonal bipyramidal Zn centres, whilst in **6**, for the linear Zn_3 unit, a central distorted octahedral zinc centre is flanked by trigonal planar and a tetrahedral zinc centres. Screening for the ring opening polymerization (ROP) of ε-caprolactone at 90 °C revealed that they are active with moderate to good conversion affording low to medium molecular weight products with at least two series of ions. For comparative studies, the trinuclear aminebis(phenolate) complex $[Zn_3(O$i-Pr$)_2L']$ (L' = *n*-propylamine-*N*,*N*-bis(2-methylene-4,6-di-*tert*-butylphenolate) **I** was prepared. Kinetics revealed the rate order **I** > **4** > **6** ≈ **2** ≈ **1** > **3**.

Received 13th May 2022,
Accepted 11th July 2022

DOI: 10.1039/d2dt01496c

rsc.li/dalton

Introduction

The search for new, greener polymers as replacements for petroleum-based plastics continues at a pace, and progress has seen biodegradable synthetic polymers applied in areas such as the biomedical field.[1] One avenue receiving much attention is the ring opening polymerization (ROP) of cyclic esters. Typically, this process requires the use of a catalyst/initiator and, when metal-based, these usually take the form of an alkoxide, or a species that can generate an alkoxide *in situ*.[2] As part of the search for catalytic systems capable of such ROP, we and others have been investigating the use of metallocalix[*n*]arenes.[3] The use of calixarenes is beneficial for a number of reasons, for example both upper and lower rims can readily be modified allowing for control over the sterics and electronics of the system as well as other properties such as solubility. Furthermore, employing calixarenes as ligands allows for the potential binding of multiple metal centres, which is attractive in terms of possible cooperative catalysis. The choice of metal is equally important, and earth-abundant metals are desirable. Given this, the metal zinc has been employed in a variety of ROP systems, usually in combination with Schiff-base type ligation, or ligands derived from diphenols.[2g,4] Moreover, a limited number of zinc-containing calix[4]arene systems have been shown to be effective ROP catalysts, suggesting such systems retain sufficient nucleophilicity at the metal.[5] Herein, we report the isolation of five trinuclear zinc complexes bearing dialkoxycalix[4]arene ligation (see Chart 1), including the serendipitous hydroxide-bridged product $[Zn_3(OH)_2(L(O)_2(O$*n*-pentyl$)_2]{\cdot}8$MeCN (**5**·8MeCN). The complex $[Zn_6(L(O$*n*-pentyl$))_2(OH)_3(C_6F_5)_3(NCMe)_3]{\cdot}3$MeCN (**6**·3MeCN), which also contains a near linear Zn_3 fragment, is also reported. Harrowfield *et al.* have reported a trimetallic zinc complex derived from *p*-*tert*-butyltetrathiacalix[4]arene.[6] We also note

[a]*Plastics Collaboratory, Department of Chemistry, University of Hull, Cottingham Road, Hull, HU6 7RX, UK. E-mail: c.redshaw@hull.ac.uk*
[b]*Chemistry Department, Loughborough University, Loughborough, Leicestershire, LE11 3TU, UK*

†Electronic supplementary information (ESI) available: molecular structure of **1′**·6MeCN, alternative view of **2**·5MeCN, molecular structure of the triclinic polymorph of $L(OH)_2(O$*n*-pentyl$)_2{\cdot}$MeCN, packing structure of $L(OH)_2(O$*n*-pentyl$)_2{\cdot}$MeCN, crystal structure data for α-$L(OH)_2(O$pentyl$)_2$, MALTI-TOF spectrum of PCL from **2** (entry 11, Table 2), MALTI-TOF spectrum of PCL from **3** (entry 14, Table 2), MALTI-TOF spectrum of PCL from **6** (entry 19, Table 2), ^{1}H NMR spectrum of PCL using **5**/BnOH (entry 17, Table 2), ^{1}H NMR spectrum ($CDCl_3$, 400 MHz, 298 K) of the PCL synthesized using **5** in the absence of BnOH (entry 18, Table 2). CCDC 2133113–2133121. For ESI and crystallographic data in CIF or other electronic format see DOI: https://doi.org/10.1039/d2dt01496c

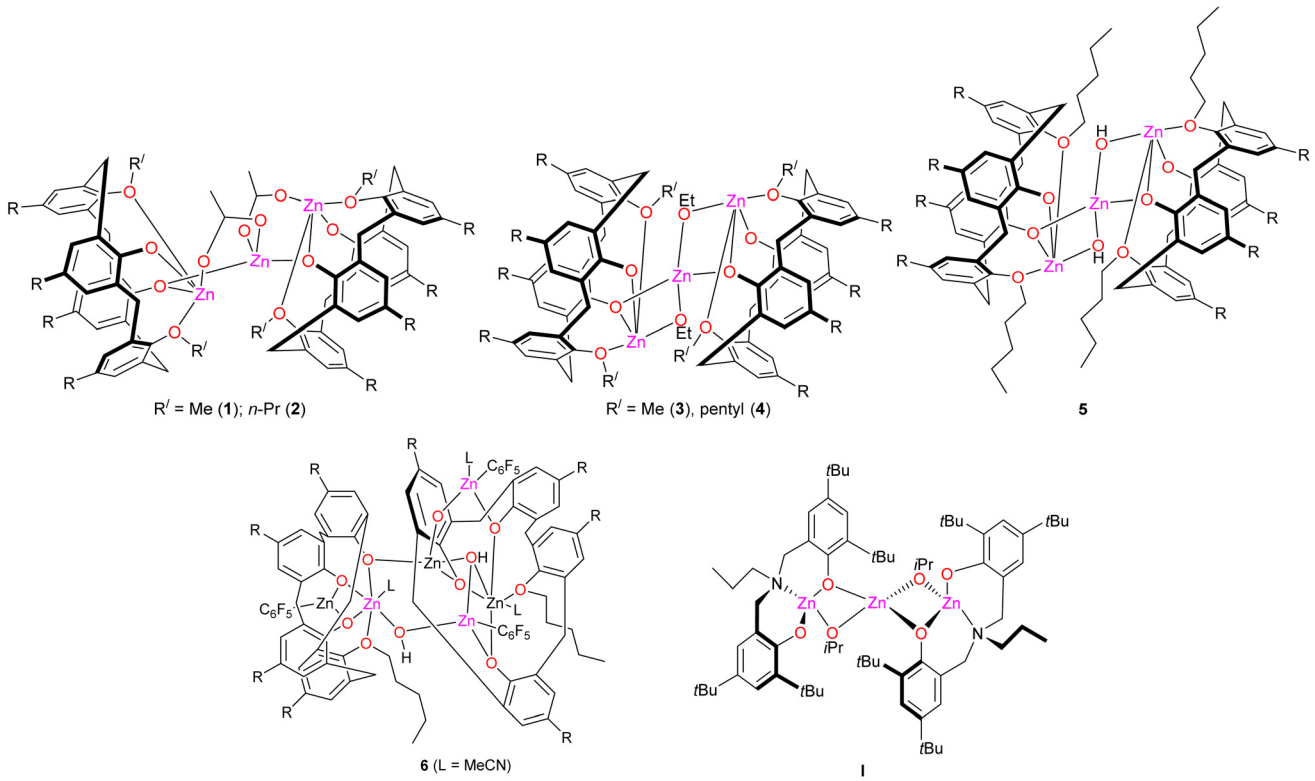

Chart 1 New pre-catalysts prepared herein (R = *t*-Bu) and I.[6]

that Ovsyannikov, Ferlay *et al.* have recently reported a trinuclear zinc complex bearing a sulfonylcalix[4]arene, however the zinc centres adopted a triangle-like arrangement.[7a] The same group have also reported the use of the sulfonylcalix[4]arene ligand set in combination with succinic acid to isolate a Zn_6 complex in which cationic trinuclear Zn_3 motifs are bridged by succinic carboxylate groups.[7b] A more linear arrangement was reported for a trimetallic zinc amino-bis(phenolate) complex **I**, which was also employed in the ROP of *rac*-lactide.[8] We also note that trinuclear zinc complexes bound by carboxylate and pyridyl ligands have recently been exploited in the ROP of ε-CL and *r*-LA.[9] Moreover, there is interest in 'trapping' zinc hydroxide/alkoxide/oxide species using organic ligands.[10]

The trinuclear zinc complexes herein have been screened for their ability to act as catalysts for the ROP of ε-caprolactone.

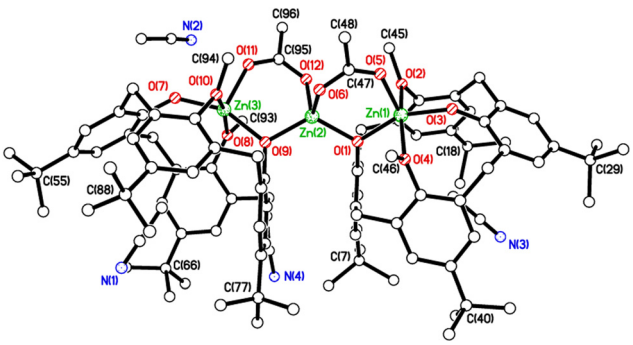

Fig. 1 Molecular structure of $[Zn_3(O_2CCH_3)_2(L(O)_2(OMe)_2)_2]\cdot 7.5MeCN$ **1**·7.5MeCN. H atoms and minor disorder components omitted for clarity. Selected bond lengths (Å) and angles (°): Zn(1)–O(1) 1.9721(13), Zn(1)–O(2) 2.1879(13), Zn(1)–O(3) 1.8656(14), Zn(1)–O(4) 2.2657(14), Zn(2)–O(1) 1.9584(13), Zn(2)–O(6) 1.9545(16), Zn(2)–O(12) 1.9498(15); Zn(1)–O(1)–Zn(2) 110.54(6), Zn(2)–O(9)–Zn(3) 111.07(6), O(1)–Zn(2)–O(9) 122.43(6).

Results and discussion

Syntheses and solid-state structures

Acetate-bridged complexes. Reaction of 1,3-dimethylether-*p*-*tert*-butylcalix[4]arene$(OH)_2$, $L(OH)_2(OMe)_2$, with $[ZnEt_2]$, and subsequent treatment with acetic acid led, following work-up, to the complex $[Zn_3(O_2CCH_3)_2(L(O)_2(OMe)_2)_2]\cdot 7.5MeCN$ (**1**·7.5MeCN). Single crystals suitable for X-ray diffraction were obtained from a saturated MeCN solution on standing (1–2 days) at ambient temperature. The molecular structure is shown in Fig. 1, with selected bond lengths and angles given in the caption. In the asymmetric unit, the whole molecule of **1**·7.5MeCN is unique. The Zn(1) and Zn(3) centres are 5-coordinate and are approximately trigonal bipyramidal (tbp) as indicated by the structural index parameters of τ = 0.06 and 0.04, respectively.[11] The central Zn(2) is 4-coordinate tetrahedral and is much less distorted than the central zinc centres found in **2** and **3** (see below). The Zn(1)–Zn(2)–Zn(3) angle is 174.539(11)°.

One MeCN resides in each of the calixarene cavities, whilst there are 5.5 other MeCNs that lie *exo* to the molecule.

From a repeat synthesis, the structure of a different solvate $[Zn_3(O_2CCH_3)_2(L(O)_2(OMe)_2)_2]\cdot 6MeCN$ (**1′**·6MeCN) has also been determined, see Fig. S1, ESI.† In the asymmetric unit, a molecule of **1′**·6MeCN lies on a 2-fold axis, so half is unique.

Use of 1,3-di-*n*-propylether-*p*-*tert*-butylcalix[4]arene$(OH)_2$, $L(OH)_2(O$*n*-$Pr)_2$, under similar conditions led, following work-up, to isolation of the complex $[Zn_3(O_2CCH_3)_2(L(O)_2(O$*n*-$Pr)_2)_2]\cdot 5MeCN$ (**2**·5MeCN). The molecular structure is shown in Fig. 2, with selected bond lengths and angles given in the caption; an alternative view is given in Fig. S2, ESI.† This is half of the asymmetric unit, so there are two metal complexes, each with a MeCN in each calixarene cavity, plus six other MeCNs *exo* to the metal complexes, three per Zn_3 complex. Data were non-merohedrally twinned *via* a 180° rotation about [0 0 1] direct & reciprocal. The twinning in conjunction with the very large structure result in the data quality being sub-optimal. However, the connectivity is clearly established as very similar to **1**. Fine details about geometry are far less reliable and should not be emphasised. Zn(1) & Zn(3) have square-based pyramidal geometry, with calixarene oxygens in the square base and an acetate oxygen apical. The central Zn(2) is tetrahedral, binding to two acetate oxygens and two calixarene phenolate oxygens, one from each calixarene. The two acetate ligands and Zn(2) provide the bridge between the two calixarenes.

These acetate-bridged complexes are soluble in common organic solvents such as MeCN, toluene, THF, acetone and dichloromethane. In toluene, the solubility of **1**·7.5MeCN is about 0.28 g per mL, whilst that of **2**·5MeCN is about 0.40 g per mL.

Ethoxide-bridged complexes. Similar treatment of $L(OH)_2(OMe)_2$ with $[ZnEt_2]$, followed by the addition of ethanol, led to the isolation of the complex

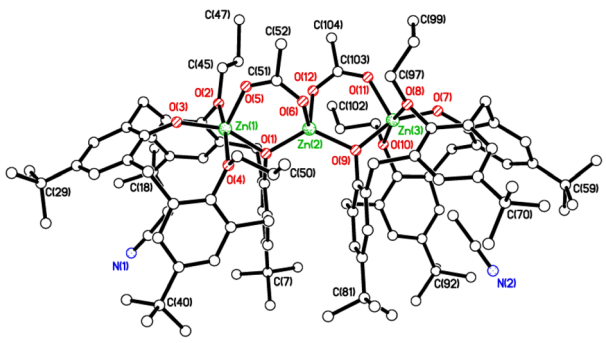

Fig. 2 Molecular structure of $[Zn_3(O_2CCH_3)_2(L(O)_2(O$*n*-$Pr)_2)_2]\cdot 5MeCN$ (**2**·5MeCN). H atoms, minor disorder components, and some MeCNs omitted for clarity. A second Zn_3 complex in the asymmetric unit has similar geometry. Selected bond lengths (Å) and angles (°): Zn(1)–O(1) 1.978(7), Zn(1)–O(2) 2.215(9), Zn(1)–O(3) 1.862(7), Zn(1)–O(4) 2.259(8), Zn(1)–O(5) 1.951(9), Zn(2)–O(1) 1.942(7), Zn(2)–O(6) 1.959(8), Zn(2)–O(9) 1.956(7), Zn(2)–O(12) 1.968(9); Zn(1)–O(1)–Zn(2) 111.0(3), Zn(2)–O(9)–Zn(3) 113.6(4), O(1)–Zn(2)–O(9) 125.1(3).

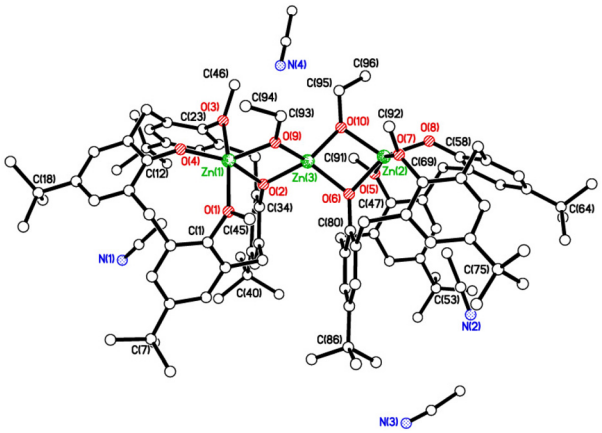

Fig. 3 Molecular structure of $[Zn_3(OEt)_2(L(O)_2(OMe)_2)_2]\cdot 4MeCN$ (**3**·4MeCN). H atoms and minor disorder components omitted for clarity. Selected bond lengths (Å) and angles (°): Zn(1)–O(1) 2.200(4), Zn(1)–O(2) 2.005(4), Zn(1)–O(3) 2.241(4), Zn(1)–O(4) 1.870(5), Zn(1)–O(9) 1.970(5), Zn(3)–O(2) 1.979(4), Zn(3)–O(6) 1.985(4), Zn(3)–O(9) 1.929(5), Zn(3)–O(10) 1.928(5); Zn(1)–O(2)–Zn(3) 97.33(18), Zn(1)–O(9)–Zn(3) 100.2(2).

$[Zn_3(OEt)_2(L(O)_2(OMe)_2)_2]\cdot 4MeCN$ (**3**·4MeCN) in good yield (*ca.* 71%). The molecular structure is shown in Fig. 3, with selected bond lengths and angles given in caption. As for **1**, there are three Zn^{2+} ions present. Each pair is bridged by one ethoxide and one phenolate oxygen of a calix[4]arene. The Zn(1) centre is 5-coordinate and approximately tbp as indicated by a structural index parameter of τ = 0.22.[11] Moreover, Zn(2) is also 5-coordinate and approximately tbp indicated by a structural index parameter of τ = 0.18.[11] The central zinc Zn(3) is distorted tetrahedral with angles in the range 81.68(18) to 114.7(2)°. The Zn(1)–Zn(3)–Zn(2) angle is 175.92(3)°. One MeCN resides in each calixarene cavity, whilst the two others are *exo* to the complex.

Reaction of the related 1,3-di-*n*-pentylether-*p*-*tert*-butylcalix[4]arene$(OH)_2$, $L(OH)_2(O$*n*-pentyl$)_2$, with $[ZnEt_2]$, followed by the addition of ethanol, led to the isolation of the complex $[Zn_3(OEt)_2(L(Opentyl)_2)_2]\cdot 4.5MeCN$ (**4**·4.5MeCN). The molecular structure is shown in Fig. 4, with selected bond lengths and angles given in the caption. As for **1**–**3**, whilst the central Zn(2) is 4-coordinate distorted tetrahedral, the other Zn centres in **4** are 5-coordinate tbp (τ = 0.296 at Zn(1) and 0.258 at Zn(3)).[11] The Zn(1)–Zn(2)–Zn(3) angle is 178.92(2)°.

These ethoxide-bridged complexes are somewhat more soluble in toluene than **1** and **2**; the solubility of **3**·4MeCN is about 0.50 g per mL and that for **4**·4.5MeCN about 1.20 g per mL.

Hydroxy-bridged complex. Interaction of $L(OH)_2(O$*n*-pentyl$)_2$, $[Zn(C_6F_5)_2]\cdot$toluene[12] and K_2CO_3 led, following work-up, to the complex $[Zn_3(OH)_2(L(O)_2(O$*n*-pentyl$)_2]\cdot 8MeCN$ (**5**·8MeCN) in low yield (<10%). The molecular structure is shown in Fig. 5, with selected bond lengths and angles given in the caption. The molecule lies on a 2-fold axis, and so half is unique. There are three Zn^{2+} ions, each pair bridged by an OH^- and a calixar-

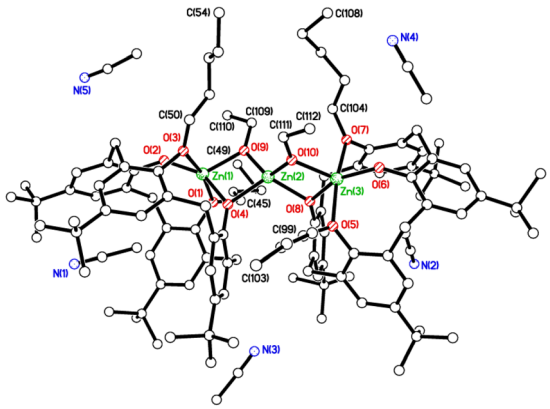

Fig. 4 Molecular structure of $[Zn_3(OEt)_2(L(O)_2(Opentyl)_2)_2]\cdot 4.5MeCN$ (**4**·4.5MeCN). H atoms and minor disorder components omitted for clarity. Selected bond lengths (Å) and angles (°): Zn(1)–O(1) 2.221(2), Zn(1)–O(2) 1.853(3), Zn(1)–O(3) 2.437(2), Zn(1)–O(4) 1.987(2), Zn(1)–O(9) 1.962(3), Zn(2)–O(4) 1.982(2), Zn(2)–O(8) 1.983(2), Zn(2)–O(9) 1.942(3), Zn(2)–O(10) 1.937(3); Zn(1)–O(4)–Zn(2) 97.14(10), Zn(1)–O(9)–Zn(2) 99.32(12), Zn(2)–O(10)–Zn(3) 99.08(11).

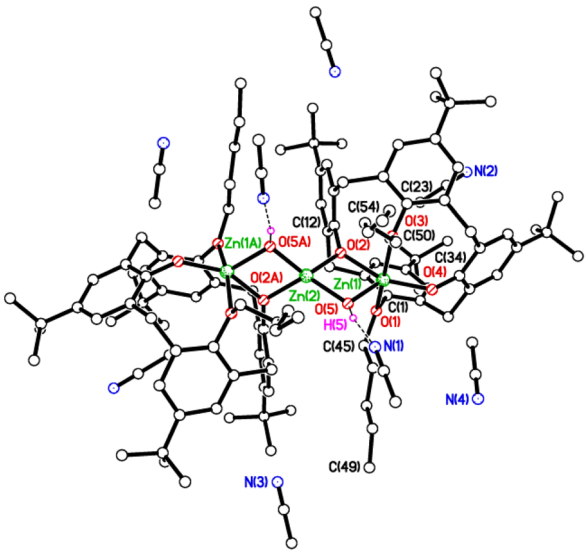

Fig. 5 Molecular structure of $[Zn_3(OH)_2(L(O)_2(On\text{-pentyl})_2]\cdot 8MeCN$ (**5**·8MeCN). H atoms, except hydroxy-H, and minor disorder components omitted for clarity. Selected bond lengths (Å) and angles (°): Zn(1)–O(1) 2.2756(14), Zn(1)–O(2) 1.9889(14), Zn(1)–O(3) 2.2587(14), Zn(1)–O(4) 1.8755(15), Zn(2)–O(2) 1.9955(14), Zn(2)–O(5) 1.9134(16); Zn(1)–O(2)–Zn(2) 95.56(6), Zn(1)–O(5)–Zn(2) 99.79(7); H-bond geometry: O(5)–H(5)···N(1) 1.98(3) Å, 170(2)°.

ene phenolate O. Zn(1) is 5-coordinate and approximately tbp indicated by a structural index parameter of $\tau = 0.25$.[11] The central Zn(2) is 4-coordinate and is very distorted from tetrahedral. The Zn(1)–Zn(2)–Zn(1A) angle is very similar to that in **1**·7.5MeCN, at 173.332(15)°. One unique MeCN hydrogen bonds to the OH^- group, one MeCN resides in the calixarene cavity and the other two MeCNs lie *exo* to the molecule. We presume the formation of **5**·8MeCN initially involves the formation of a bimetallic $\{[Zn(C_6F_5)]_2L(O)(Opentyl)_2\}$ species which then undergoes a fortuitous hydrolysis reaction to form the hydroxide-bridged product **5**·8MeCN. Attempts to prepare **5** *via* the addition of H_2O to intermediate alkylzinc $L(O)_2(Opentyl)_2$ species led only to the isolation of the parent calixarene ligand, namely $L(OH)_2(On\text{-pentyl})_2$. The molecular structures of two polymorphs of $L(OH)_2(On\text{-pentyl})_2\cdot MeCN$ are given in the ESI (Fig. S3, S4 and Table S1†). A new triclinic β polymorph crystallises in space group $P\bar{1}$ with $Z' = 2$. We have previously reported the α monoclinic polymorph which crystallises in space group $P2_1/n$ with $Z' = 1$, which was obtained again during the present studies, and for which we now report a considerably more precise determination.[13] In both polymorphs an acetonitrile molecule resides in the calixarene cavity.

Reaction of commercial $[Zn(C_6F_5)_2]$ with $L(OH)_2(On\text{-pentyl})_2$ in the presence of K_2CO_3 led, following work-up (MeCN), to the colourless complex $[Zn_6(L(On\text{-pentyl}))_2(OH)_3(C_6F_5)_3(NCMe)_3]\cdot 3MeCN$ (**6**·3MeCN). This is the asymmetric unit. There are 12 positive charges, from the 6 Zn^{2+} ions, balanced by 2 calixarenes each with three negative charges, 3 $C_6F_5^-$ anionic ligands, and three OH^- ions. The two calixarenes having different conformations (pinched and cone), see Fig. 6. The pinched cone houses a C_6F_5 ligand bound to Zn(6), while the conventional cone has an MeCN ligand bound to Zn(1) in the cavity. For the pinched cone, the opposite *para* C atoms in the rings, namely C(53) and C(75), are 7.130(5) Å apart, while the other pair, C(64) and C(86), are 10.715(5) Å apart. In the conventional cone, the two comparable distances are 7.956(6) Å for C(4) to C(26), and 8.015(5) Å for C(15) to C(37). The Zn(1) and Zn(5) centres are 6-coordinate octahedral, while Zn(6), in the pinched cone cavity, is 3-coordinate trigonal planar, but may be forming π-interactions with the nearby pair of calixarene aromatic rings bound to O(5) and O(7). The centres Zn(2), Zn(3), and Zn(4) are all 4-coordinate distorted tetrahedral. In the core, there are three Zn_2O_2 diamond motifs, with that involving Zn(5) and Zn(6) utilising two calixarene phenolate oxygens. Those involving Zn(1)/Zn(2) and Zn(1)/Zn(4) are linked, and involve one calixarene phenolate oxygen and the shared hydroxyl at O(9). There are also three Zn_3O_3 ring motifs, with that involving Zn(2)/Zn(4)/Zn(5) including two phenolate oxygens from different calixarenes and an OH^-, while the two involving Zn(1)/Zn(3)/Zn(4) include two phenolate oxygens from the same conventional cone calixarene and an OH^-, or two OH^- ligands and one phenolate oxygen. Indeed, only the two calixarene oxygens bearing the pentyl groups are not involved in these ring motifs. In terms of a linear Zn_3 fragment, the angles subtended at Zn(5), with Zn(2) and Zn(6) on either side, is 162.75(2)°.

There is intramolecular bifurcated H-bonding from the OH^- ligand (O(9), which does not H-bond to an MeCN) to two F atoms of two different C_6F_5 ligands. Of the 3 molecules of MeCN of crystallization, two H-bond to OH^- groups, whilst the other lies *exo* to the metal complex.

Key structural parameters for the calixarenes **1–6** are presented in Table 1.

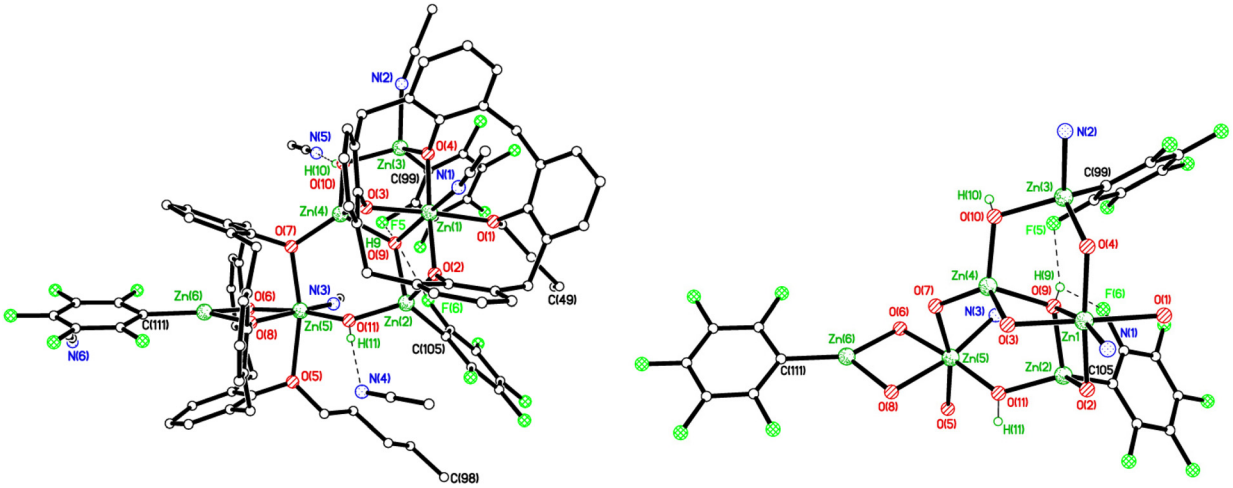

Fig. 6 Molecular structure of $[Zn_6(L(On\text{-pentyl}))_2(OH)_3(C_6F_5)_3(NCMe)_3]\cdot 3MeCN$ (**6**·3MeCN). Calixarene *t*Bu groups, and H atoms except hydroxy-H have been omitted for clarity. The right-hand image shows the core of the molecule. Selected bond lengths (Å) and angles (°): Zn(1)–O(1) 2.207(3), Zn(1)–O(2) 1.996(2), Zn(1)–O(3) 2.033(3), Zn(1)–O(4) 2.014(3), Zn(1)–O(9) 2.184(3), Zn(1)–N(1) 2.180(3), Zn(2)–O(2) 1.986(2), Zn(2)–O(9) 2.045(3), Zn(2)–O(11) 1.915(3), Zn(2)–C(105) 2.007(4), Zn(3)–O(10) 1.947(3), Zn(3)–N(2) 2.087(4), Zn(4)–O(3) 1.948(2), Zn(4)–O(7) 1.898(2), Zn(4)–O(9) 2.021(3), Zn(4)–O(10) 1.929(3), Zn(5)–O(5) 2.335(2), Zn(5)–O(6) 2.069(3), Zn(5)–O(7) 2.082(2), Zn(5)–O(8) 2.031(2), Zn(5)–O(11) 1.921(3), Zn(5)–N(3) 2.167(3), Zn(6)–O(6) 1.914(2), Zn(6)–O(8) 1.900(3), Zn(6)–C(111) 1.950(4); Zn(1)–O(1)–Zn(2) 100.87(11), Zn(2)–O(11)–Zn(5) 128.10(14), Zn(5)–O(6)–Zn(6) 100.23(10). H-bond geometry: O(9)–H(9)···F(5) 2.28(2) Å, 158(4)°, O(9)–H(9)···F(6) 2.27(3) Å, 125(3)°, O(10)–H(19)···N(5) 2.08(2) Å, 109(4)°, O(11)–H(11)···N(4) 2.19(2) Å, 174(4)°.

Table 1 Key structural data for **1**–**6**

Compound	**1**·8MeCN	**2**·5MeCN	**3**·4MeCN	**4**·4.5MeCN	**5**·8MeCN	**6**·3MeCN
Coordination number						
Zn(1)	5	5	5	5	5	—
Zn(2)	4	4	5	4	4	4
Zn(3)	5	5	4[a]	5	5	—
Zn(4)	—	—	—	—	—	—
Zn(5)	—	—	—	—	—	6
Zn(6)	—	—	—	—	—	3
Geometry						
Zn(1)	tbp (τ = 0.06)[b]	Tetragonal pyramid	tbp (τ = 0.22)[b]	tbp (τ = 0.296)[b]	tbp (τ = 0.25)[b]	—
Zn(2)	Tetrahedral	Tetrahedral	tbp (τ = 0.18)[b]	Tetrahedral	Tetrahedral	Tetrahedral
Zn(3)	tbp (τ = 0.04)[b]	Tetragonal pyramid	Tetrahedral	tbp (τ = 0.258)[b]	tbp (τ = 0.25)[b]	—
Zn(4)	—	—	—	—	—	—
Zn(5)	—	—	—	—	—	Octahedral
Zn(6)	—	—	—	—	—	Trigonal planar
Linearity of Zn_3 motif	175°	174°	176°	179°	173°	163°

[a] Note this is the central zinc. [b] tbp = trigonal bipyramid; Reedijk *et al.* defined τ as $\tau = (p - r)/60$ which is applicable to five-co-ordinate structures as an index of the degree of trigonality.[11]

Ring opening polymerization studies

Based on our previous zinc calixarene ROP studies,[4b] we selected the conditions of 90 °C with a ratio of ε-CL to complex of 500 : 1 in the presence of one equivalent of benzyl alcohol over 24 h. For comparative studies, we also screened the known trinuclear complex **I**, which bears the aminebis(phenolate) ligand *n*-propylamine-*N*,*N*-bis(2-methylene-4,6-di-*tert*-butylphenolate).[8] Data for the runs are presented in Table 2, where [Cat] represents the concentration of the complex employed, and it can be seen that low to medium molecular weight products are formed with good control. Interestingly, despite the narrow PDI values, MALDI-TOF spectra revealed at least two series of ions corresponding to polycaprolactone (PCL). For example, in Fig. S5 (for **2**, entry 11, Table 2, ESI) and S6 (for **3**, entry 14, Table 2, ESI),† the lower mass species is consistent with sodiated PCL with H/OH end groups. The OH end group likely forms an effective carboxylic acid end group with a carbonyl from the last repeat unit that can exchange the acidic proton with sodium, resulting in the higher mass sodiated series. Cyclic polymers are also evident, see ESI.† In the case of **6** (entry 19, Table 2), in the MALDI-TOF spectrum (Fig. S7, ESI†) there appear to be groups of three main series and so BnO–/–H end groups should correspond to

Table 2 Synthesis of polycaprolactone using complexes **1–6** and **I**

Entry	Cat.	[Monomer] : [Cat] : BnOH	T/°C	t/h	Conv[a] (%)	M_n[b]	$M_{n,Cal}$[c]	PDI[d]
1	**1**	500 : 1 : 2	90	24	79.7	11 870	45 590	1.18
2	**1**	500 : 1 : 0	90	24	50.7	43 440	29 040	1.44
3	**1**	100 : 1 : 2	90	24	96	6980	11 060	1.37
4	**1**	250 : 1 : 2	90	24	99	14 790	28 350	1.29
5	**1**	1000 : 1 : 2	90	24	99	3860	113 100	1.16
6[e]	**1**	500 : 1 : 2	90	24	5.7	910	3360	1.12
7	**1**	500 : 1 : 2	90	1	38.3	6790	21 960	1.23
8	**1**	500 : 1 : 2	90	3.5	97	22 430	55 460	1.25
9	**1**	500 : 1 : 2	90	5	99	21 030	56 600	1.32
10	**1**	500 : 1 : 2	15	24	5.5	2160	3240	1.08
11	**2**	500 : 1 : 0	90	24	48.1	3260	27 550	1.31
12	**2**	500 : 1 : 2	90	24	58.4	3520	33 430	1.16
13	**3**	500 : 1 : 1	90	24	99.7	2895	57 000	1.11
14	**3**	500 : 1 : 0	90	24	>99	2760	56 600	1.09
15	**4**	500 : 1 : 0	90	24	>99	21 275	56 600	2.59
16	**4**	500 : 1 : 2	90	24	>99	34 690	56 600	2.30
17	**5**	500 : 1 : 2	90	24	>99	29 765	56 600	2.25
18	**5**	500 : 1 : 0	90	24	56.9	19 070	32 580	2.10
19	**6**	500 : 1 : 1	90	48	97.5	5940	55 750	1.25
20	**I**	500 : 1 : 0	20	24	29	4750	16 650	1.24
21	**I**	500 : 1 : 0	90	24	99.5	17 390	56 890	1.98

[a] Conversion was confirmed by ^{1}H NMR spectroscopy. [b] Determined by GPC analysis calibrated with polystyrene standards and multiplied by correction factor of 0.56. [c] F.W.[M]/[BnOH] (conversion) + BnOH. [d] Polydispersity index (M_w/M_n) were determined by GPC. [e] Conducted in air.

the first series in each group *i.e.* m/z 4356, 4470, 3585, 4698, *etc*. Based on the average masses and inter-series mass differences, the middle series (m/z 4380, 4494, 4608, 4722, *etc*.) is likely to have HO–/–H end groups and the third series (m/z 4394, 4507, 4622, 4736, *etc*.) is likely CH_3O–/–H end groups. For runs employing BnOH, end group analysis by ^{1}H NMR spectroscopy (*e.g.* Fig. S8† for entry 17, Table 2) is consistent with the presence of a BnO end group (*cf.* Fig. S9† for entry 18, Table 2). From a kinetic study (Fig. 7) of **1–6** (not **5**) and **I**, conducted in the presence of two equivalents of BnOH, it was observed that the polymerization rate exhibited first-order dependence on the ε-CL concentration (Fig. 7(a)), and the conversion of monomer achieved over 150 min was >70% for **I** and **4**, whereas for the other systems, the conversion was <50% over 300 min.

The activity trend in this case revealed that **I** was the most active and then **4** > **6** ≈ **2** ≈ **1** > **3**. Complex **I** is thought to be more active given the more open (*i.e.* less sterically congested) environment around the three 4-coordinate tetrahedral zinc centres, which contrasts with the tbp geometries exhibited by two of the Zn centres found in the Zn_3 calixarene complexes. Given that the NMR data suggests the solid-state structures are retained in solution, we have examined the structural data. In addition to that presented in Table 1, for **1–5**, the Zn–O bond lengths to the alkylated Os are longer than to the non-alkylated Os, which generates a small distortion in the cone conformation. Looking at all the cross-cone distances C(4)–C(26) and C(15)–C(37) (and their equivalents on the other calixarenes), there is one set of short distances [7.3–7.9 Å] and one longer set [7.9–8.6 Å]. In the case of the most active complex **4**, it pos-

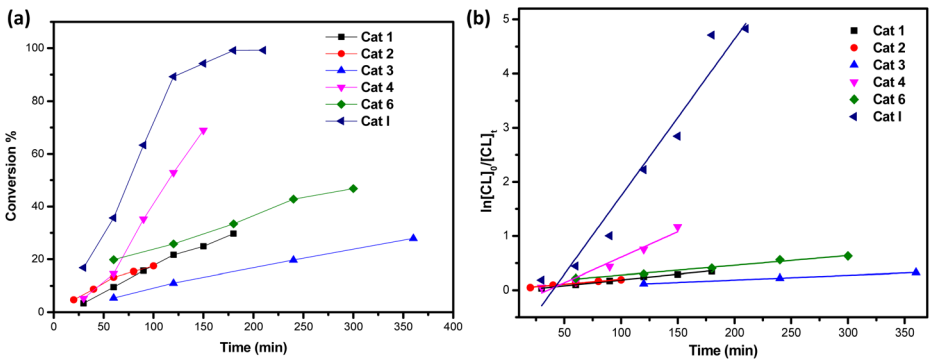

Fig. 7 (a) Relationship between conversion and time for the polymerization of ε-CL by using complexes **1–6** (not **5**) and **I**; (b) plot of $\ln[CL]_0/[CL]_t$ *vs*. time for the polymerization of ε-CL by using complexes **1–6** (not **5**) and **I**.

sesses both the smallest and largest of these distances [7.311 and 8.594 Å] on the lower numbered cone. It is thought that this distortion allows the Zn centre to be more accessible, which combined with the higher solubility of **4** leads to the observed higher activity. Complex **6** also possesses asymmetric calixarene cones, and this, together with the presence of the labile MeCN ligands, is thought to be the reason for its high observed activity. The activities of the two acetate complexes **1** and **2** are similar, despite the differing R′ groups at the lower rim, but both are slightly more active than the ethoxide-bridged complex **3**.

Conclusions

In conclusion, we have isolated and structurally characterized a number of rare examples of trinuclear zinc-bearing 1,3-dialkoxycalix[4]arene ligands. The formation of products such as **5** from fortuitous syntheses suggests that the adoption of such trinuclear structures is thermodynamically driven. The products are capable of the ROP of ε-caprolactone affording low to medium molecular weight products. The products contain multiple series of ions with a variety of end groups and can contain either cyclic or linear species, or both. The congested geometries at the outer zinc centers in the calixarene complexes, compared with those in the complex **I** bearing the aminebis(phenolate), results in a slower ROP process.

Experimental

General

All manipulations were carried out under an atmosphere of dry nitrogen using Schlenk and cannula techniques or in a conventional nitrogen-filled glove box. Ethanol was dried over molecular sieves (3 Å). Toluene was dried over sodium, acetonitrile and triethylamine were dried over calcium hydride, and dmso and acetone were dried over molecular sieves. All solvents were distilled and degassed prior to use. ε-Caprolactone was stored over activated 4 Å molecular sieves and then distilled prior to use. Benzyl alcohol was distilled, and then a stock solution prepared containing 0.01 mmol per mL. Compound **I** was made by the method of Kozak.[8] $[Zn(C_6F_5)_2]$·toluene was made by the method of Bochmann.[12] All other chemicals were purchased from Sigma-Aldrich or TCI UK and used as received. IR spectra (Nujol mulls, KBr windows) were recorded on a Nicolet Avatar 360 FT IR spectrometer. Matrix Assisted Laser Desorption/Ionization Time of Flight (MALDI-TOF) mass spectrometry was performed in a Bruker autoflex III smart beam in linear mode, and the spectra were acquired by averaging at least 100 laser shots. 2,5-Dihydroxybenzoic acid was used as the matrix and THF as solvent. Sodium chloride was dissolved in methanol and used as the ionizing agent. Samples were prepared by mixing 20 μL of matrix solution in THF (2 mg mL^{-1}) with 20 μL of matrix solution (10 mg mL^{-1}) and 1 μL of a solution of ionizing agent (1 mg mL^{-1}). Then 1 mL of these mixtures was deposited on a target plate and allowed to dry in air at ambient temperature. Elemental analyses were performed by the elemental analysis service at the London Metropolitan University, the Department of Chemistry & Biochemistry, University of Hull, and at Nanjing University of Information Science & Technology.

Synthesis of $[Zn_3(O_2CCH_3)_2(L(O)_2(OMe)_2)_2]$·7.5MeCN (1·7.5MeCN). $ZnEt_2$ (2.96 mL, 1.0 M, 2.96 mmol) was added to $L^4(OH)_2(OMe)_2$ (1.00 g, 1.48 mmol) in toluene (30 mL) and the system was refluxed for 12 h. On cooling, acetic acid (0.17 mL, 3.0 mmol) was added and the system was stirred for 12 h. The volatiles were then removed *in vacuo*, and the residue was extracted into hot MeCN (30 mL). On standing at ambient temperature (1–2 days), colourless prisms of **1**·7.5MeCN formed (0.93 g, 63%). $C_{98}H_{125}Zn_3NO_{12}$ (−6.5MeCN) requires C 69.03, H 7.39, N 0.82%. Found C 68.80, H 7.82, N 0.87%. IR: 3456w, 3342bm, 3179bw, 1681m, 1596w, 1297s, 1261s, 1208s, 1168m, 1100m, 1017s, 987m, 943w, 920w, 871m, 802s, 722s, 634w. ^{1}H NMR ($CDCl_3$) δ: 7.08 (AB quarter, J = 7.8 Hz, J' = 2.4 Hz, 4H, aryl*H*), 7.00 (overlapping d, J = 2.8 Hz, 2H, aryl*H*), 6.92 (AB quartet, J = 12.2 Hz, J' = 2.4 Hz, 4H, aryl*H*), 6.82 (d, J = 2.4 Hz, 2H, aryl*H*), 6.72 (d, J = 2.8 Hz, 2H, aryl*H*), 5.15 (d, J = 12.4 Hz, 2H, *endo*-CH_2), 4.47 (d, J = 12.4 Hz, 2H, *endo*-CH_2), 4.38 (d, J = 12.0 Hz, 2H, *endo*-CH_2), 4.23 (s, 6H, OCH_3), 3.86 (s, 6H, OCH_3), 3.33 (overlapping d, J = 12.4 Hz, 4H, *endo*- + *exo*-CH_2), 3.24 (d, J = 12.0 Hz, 2H, *exo*-CH_2), 3.17 (d, J = 12.0 Hz, 2H, *exo*-CH_2), 2.39 (s, 6H, O*Ac*), 2.16 (d, J = 12.8 Hz, 2H, *exo*-CH_2), 1.27 (s, 18H, $C(CH_3)_3$), 1.19 (s, 18H, $C(CH_3)_3$), 1.17 (s, 18H, $C(CH_3)_3$), 1.12 (s, 18H, $C(CH_3)_3$). The other solvate, namely **1′**·6MeCN, was prepared as above.

Synthesis of $[Zn_3(O_2CCH_3)_2(L(O)_2(O$*n*-Pr)$_2)_2]$·5MeCN (2·5MeCN). As for **1**, but using $ZnEt_2$ (2.73 mL, 1.0 M, 2.73 mmol), $L^4(OH)_2(O$*n*-Pr$)_2$ (1.00 g, 1.36 mmol) and acetic acid (0.17 mL, 3.0 mmol) affording **2** as a white crystalline solid (1.10 g, 75%). $C_{104}H_{138}Zn_3O_{12}$ (sample dried *in vacuo* for 3 h, −5MeCN) requires C 70.32, H 7.83%. Found C 70.30, H 8.40%. IR: 2247w, 1573s, 1364s, 1323w, 1306s, 1261s, 1244w, 1196s, 1125m, 1090m, 1062w, 1025m, 989w, 953w, 947w, 936w, 917w, 907w, 889w, 868m, 836w, 820m, 800s, 750w, 722m, 670w, 636w, 619w, 523w. ^{1}H NMR ($CDCl_3$) δ: 8.13 (m, 2H, aryl*H*), 7.15 (s, 1H aryl*H*), 7.02 (m, 1H aryl*H*), 6.92 (m, (s, 6H aryl*H*), 6.85 (d, J = 2.8 Hz, 1H, aryl*H*), 5.25 (d, J = 12.4 Hz, 2H, *endo*-CH_2), 4.56 (m, 2H, OCH_2), 4.36 (d, J = 11.6 Hz, 2H, *endo*-CH_2), 4.30 (d, J = 12.8 Hz, 4H, *endo*-CH_2), 4.18 (m, 2H, OCH_2), 4.04 (m, 2H, OCH_2), 3.82 (m, 2H, OCH_2), 3.31 (d, J = 12.8 Hz, 2H, *exo*-CH_2), 3.26 (d, J = 12.0 Hz, 2H, *exo*-CH_2), 3.17 (d, J = 12.0 Hz, 2H, *exo*-CH_2), 3.14 (d, J = 12.0 Hz, 2H, *exo*-CH_2), 2.24 (s, 6H O*Ac*), 2.06 (m, 6H, $OCH_2CH_2CH_3$), 1.66 (m, 2H, $OCH_2CH_2CH_3$), 1.29 (s, 6H, MeCN), 1.24 (s, 18H, $C(CH_3)_3$), 1.19 (s, 18H, $C(CH_3)_3$), 1.16 (s, 18H, $C(CH_3)_3$), 1.12 (s, 18H, $C(CH_3)_3$), 1.06 (s, 6H, MeCN), 1.03 (s, 3H, MeCN), 0.99 (t, J = 7.2 Hz, 6H, CH_3), 0.89 (t, J = 7.2 Hz, 6H, CH_3). Mass spec. (MALDI): 1717 ((M − 5MeCN − OAc).

Synthesis of $[Zn_3(OEt)_2(L(O)_2(OMe)_2)_2]$·4MeCN (3·4MeCN). As for **1**, but using $L^4(OH)_2(OMe)_2$ (1.00 g, 1.48 mmol) [$ZnEt_2$]

(2.96 ml, 1.0 M, 2.96 mmol) and EtOH (0.17 mL, 3.0 mmol) affording colourless prisms (0.94 g, 71%). $C_{100}H_{131}Zn_3N_2O_{10}$ (sample dried *in vacuo* for 2 h, −2MeCN) requires C 69.94, H 7.69, N 1.63%. Found C 68.52, H 7.59, N 1.59%. IR: 3457w, 3319bm, 3180w, 2247w, 1681m, 1664m, 1586m, 1482s, 1364s, 1299s, 1260s, 1207s, 1168m, 1124m, 1101m, 1092m, 1005s, 946w, 870m, 785s, 764w, 755w, 722w, 671w, 637w. ^{1}H NMR (C_6D_6) δ: 7.26 (bm, 4H, aryl*H*), 7.20 (m, 2H, aryl*H*), 7.07 (bm, 1H, aryl*H*), 7.03 (bm, 3H, aryl*H*), 6.93 (bm, 4H, aryl*H*), 4.77 (bq, 4H, *J* obscured, OCH_2CH$_3$), 4.49 (d, 2H, *J* = 14.4 Hz, *endo*-CH_2), 4.41 (d, 2H, *J* = 12.4 Hz, *endo*-CH_2), 3.86 (s, 6H, O*Me*), 3.77 (d, 2H, *J* = 12.4 Hz, *endo*-CH_2), 3.41 (s, 6H, O*Me*), 3.37 (overlapping d, 6H, *endo* + *exo*-CH_2), 3.21 (d, 2H, *J* = 12.0 Hz, *exo*-CH_2), 3.08 (d, 2H, *J* = 12.8 Hz, *exo*-CH_2), 1.84 (t, 6H, *J* = 6.8 Hz, OCH$_2$CH_3), 1.47 (s, 18H, C(CH_3)$_3$), 1.24 (s, 18H, C(CH_3)$_3$), 0.93 (s, 18H, C(CH_3)$_3$), 0.84 (s, 18H, C(CH_3)$_3$), −0.32 (s, 6H *Me*CN). Mass spec. (MALDI): 1525 (M − 4MeCN − Zn − OEt), 1413 (M − 4MeCN − 2Zn − 2OEt).

Synthesis of [Zn$_3$(OEt)$_2$(L(Opentyl)$_2$)$_2$]·4.5MeCN (4·4.5MeCN). As for **1**, but using L^4(OH)$_2$(O*n*-pentyl)$_2$ (1.00 g, 1.27 mmol), [ZnEt$_2$] (2.54 ml, 1.0 M, 2.54 mmol) and EtOH (0.15 mL, 2.5 mmol) affording colourless prisms. Yield: 1.03 g, 79%. $C_{117}H_{165.5}N_{2.5}Zn_3O_{10}$ (sample dried *in vacuo* for 2 h, −2MeCN) requires C 71.58, H 8.50, N 1.78%. Found C 71.80, H 8.94, N 1.73%. IR: 2288w, 2248w, 1746w, 1584m, 1189s, 1172m, 1125s, 1110s, 1093s, 1045s, 1025m, 980s, 947w, 937w, 917w, 900w, 891w, 871s, 825m, 801s, 763w, 723m, 670w, 635w, 591w, 538m, 502w, 458w, 429w. Mass spec. (MALDI): 1133 (M − 3MeCN − L(Opentyl)$_2$), 1092 (M − 3MeCN − L(Opentyl)$_2$). ^{1}H NMR (C_6D_6) δ: 7.25 (bm, 4H aryl*H*), 7.21 (s, 1H, aryl*H*), 7.16 (bm, 4H, aryl*H*), 7.10 (bm, 6H, aryl*H*), 6.97 (s, 1H, aryl*H*), (4.89m, 4.69m 4.49 d, 4.20 bm, 4.08 bm; 16H, *endo*-CH_2 + 4× OCH_2), (3.81 overlapping d, 3.70m, 3.50bm, 3.33bm; 12H, *exo*-CH_2 + 2× OCH_2), 1.46 (s, 18H, C(CH_3)$_3$), 1.39 (m, 4H, CH_2-pentyl), 1.32 (m, 2H, CH_2-pentyl), 1.29 (s, 18H, C(CH_3)$_3$), 1.27–1.07 (overlapping m, 10H, CH_2-pentyl), 1.02, (s, 36H, C(CH_3)$_3$), 0.93 (overlapping m, 6H, CH_3), 0.83 (m, 6H, CH_3).

Synthesis of [Zn$_3$(OH)$_2$(L(O)$_2$(O*n*-pentyl)$_2$]·8MeCN (5·8MeCN). As for **1**, but using L(OH)$_2$(O*n*-pentyl)$_2$ (1.00 g, 1.27 mmol) [Zn(C$_6$F$_5$)$_2$]·toluene (1.01 g, 2.54 mmol) and K_2CO_3 (0.06 g, 0.43 mmol) affording colourless prisms. Yield: 0.16 g, 8.8%. $C_{118}H_{165}Zn_3N_5O_{10}$ (sampled dried for 2 h *in vacuo*, −3MeCN) requires C 70.52, H 8.28, N 3.45%. Found C 69.82, H 8.66, N 2.70%. IR: 3387bs, 3176w, 1598w, 1303s, 1260s, 1241m, 1195s, 1170m, 1097s, 1076m, 999s, 980m, 946w, 919w, 893m, 801s, 722s, 635w.

Synthesis of [Zn$_6$(L(O*n*-pentyl))$_2$(OH)$_3$(C$_6$F$_5$)$_3$(NCMe)$_3$]·3MeCN (6·3MeCN). As for **1**, but using L(OH)$_2$(O*n*-pentyl)$_2$ (1.00 g, 1.27 mmol) [Zn(C$_6$F$_5$)$_2$] (1.01 g, 2.54 mmol) and K_2CO_3 (0.06 g, 0.43 mmol) affording pale yellow crystals (0.81 g, 73%). $C_{122}H_{138}F_{15}Zn_6N_3O_{11}$ (sample dried *in vacuo* for 2 h, −3MeCN) requires C 58.62, H 5.57, N 1.68%. Found C 57.23, H 5.89, N 1.46%. IR: 3352bm, 1659w, 1598w, 1533w, 1503m, 1363s, 1301m, 1261s, 1204s, 1123s, 1097s, 1048s, 1023s, 962w, 951m, 919w, 871m, 801s, 722m, 635w, 527w. ^{1}H NMR (C_6D_6) δ: 8.96 (s, 1H, O*H*), 8.72 (s, 2H, O*H*), 7.29 (s, 1H, aryl*H*), 7.16 (m, 2H, aryl*H*), 7.13 (m, 2H, aryl*H*), 7.08 (overlapping m, 4H, aryl*H*), 7.04 (m, 2H, aryl*H*), 6.99 (m, 1H, aryl*H*), 6.90 (s, 4H, aryl*H*), 4.64 (d, 2H, *J* = 13.2 Hz, *endo*-CH_2), 4.47 (overlapping d, 5H, *endo*-CH_2), 3.72 (m, 4H, OCH_2 of pentyl), 3.37 (overlapping d, 6H, *exo*-CH_2), 3.29 (d, 2H, *J* = 12.4 Hz, *exo*-CH_2), 1.89 (m, 4H, CH_2 of pentyl), 1.54 (m, 4H, CH_2 of pentyl), 1.40 (s, 18H, C(CH_3)$_3$), 1.39 (s, 9H, C(CH_3)$_3$), 1.30 (overlapping m, 4H, CH_2 of pentyl) 1.19 (s, 9H, C(CH_3)$_3$), 1.11 (s, 9H, C(CH_3)$_3$), 0.94 (t, 3H, *J* = 7.2 Hz, CH_3 of pentyl), 0.84 (t, 3H, *J* = 7.2 Hz, CH_3 of pentyl), 0.83 (s, 18H, C(CH_3)$_3$), 0.61 (s, 9H, C(CH_3)$_3$), −0.20 (bs, 9H, *Me*CN). ^{19}F NMR (C_6D_6) δ: −113.65, −138.99, −153.99, −155.12, −157.78, −160.32, −162.18, −162.20.

Procedure for ROP

Typical polymerization procedure in the presence of one equivalent of benzyl alcohol (Table 2, entry 1) is as follows. A toluene solution of **1** (0.01 mmol, in 1.0 mL toluene) and, if required, BnOH (0.02 mmol) were added into a Schlenk tube in the glove-box at room temperature. The solution was stirred for 2 min, and then ε-caprolactone (typically 5 mmol unless stated otherwise) along with 1.5 mL toluene was added to the solution. The reaction mixture was then placed into an oil bath pre-heated to the required temperature, and the solution was stirred for the prescribed time. The polymerization mixture was then quenched by addition of an excess of glacial acetic acid (0.2 mL) into the solution, and the resultant solution was then poured into methanol (200 mL). The resultant polymer was then collected on filter paper and was dried *in vacuo*.

Kinetic studies

The polymerizations were carried out at 130 °C in toluene (2 mL) using 0.010 mmol of complex. The molar ratio of monomer to initiator to co-catalyst was fixed at 500 : 1 : 2, and at appropriate time intervals, 0.5 μL aliquots were removed (under N_2) and were quenched with wet $CDCl_3$. The percent conversion of monomer to polymer was determined using ^{1}H NMR spectroscopy.

X-ray crystallography

The diffraction data were collected at low temperature on either sealed tube or rotating anode systems, or in the case of **5**·8MeCN using synchrotron radiation at Daresbury Laboratory Station 9.8.[14,15] All data sets were corrected for absorption, Lp effects and, where significant, for extinction effects. CCD or hybrid pixel array detectors were employed. Structures were solved by direct methods or *via* a charge flipping algorithm and all non-H atoms were refined anisotropically.[16,17] H atoms were constrained except those on hetero atoms if the data quality allowed. Further details are provided in Table 3, in the deposited cif files, and the ESI.† Non-routine aspects are described below for each structure. Where disorder was modelled, this was supported by using geometric and anisotropic displacement parameter restraints.

For **1**·7.5MeCN: *t*Bu groups C(40), C(55), and C(66) within the calix[4]arene ligands were modelled with their methyl

Table 3 Crystal structure data for **1**·7.5MeCN, **1′**·6MeCN, **2**·5MeCN, **3**·4MeCN, **4**·4.5MeCN, **5**·8MeCN, **6**·3MeCN, and $L(OH)_2(Opentyl)_2$

Compound	**1**·7.5MeCN	**1′**·6MeCN	**2**·5MeCN	**3**·4MeCN
Formula	$C_{111}H_{144.5}Zn_3N_{7.50}O_{12}$	$C_{108}H_{140}Zn_3N_6O_{12}$	$C_{114}H_{153}Zn_3N_5O_{12}$	$C_{104}H_{137}Zn_3N_4O_{10}$
Formula weight	1971.94	1910.36	1981.51	1799.28
Crystal system	Monoclinic	Monoclinic	Triclinic	Monoclinic
Space group	$P2_1/c$	$I2/a$	$P\bar{1}$	$P2_1/c$
Unit cell dimensions				
a (Å)	18.65096(9)	22.336(2)	18.5416(2)	12.3700(15)
b (Å)	23.45772(11)	19.6856(18)	23.5115(3)	22.934(3)
c (Å)	25.30949(11)	23.872(4)	25.1000(3)	18.132(2)
α (°)	90	90	91.7320(11)	90
β (°)	105.0808(11)	90.4320(12)	90.6899(10)	106.849(2)
γ (°)	90	90	93.3356(10)	90
V (Å^3)	10691.77(10)	10 496(2)	10917.5(2)	4923.1(10)
Z	4	4	4	2
Temperature (K)	100(2)	150(2)	100(2)	150(2)
Wavelength (Å)	1.54178	0.71073	1.54178	0.71073
Calculated density (g cm^{-3})	1.225	1.209	1.206	1.214
Absorption coefficient (mm^{-1})	1.27	0.74	1.24	0.78
Crystal size (mm^3)	0.10 × 0.09 × 0.04	0.35 × 0.15 × 0.15	0.16 × 0.10 × 0.06	0.46 × 0.26 × 0.05
θ (max.) (°)	70.5	28.3	68.5	25.0
Reflections measured	220 405	53 490	311 775	39 466
Unique reflections	20 337	13 090	91 977	17 245
Reflections with $I > 2\sigma(I)$	18 519	9277	70 748	13 412
R_{int}	0.042	0.053	0.196	0.052
Number of parameters	1164	654	2542	1247
R_1 [$F^2 > 2\sigma(F^2)$]	0.041	0.053	0.172	0.049
wR_2 (all data)	0.118	0.146	0.492	0.118
GOOF, S	1.05	1.02	1.08	1.00
Largest difference peak and hole (e Å^{-3})	0.63 and −0.65	1.15 and −0.59	2.85 and −1.40	0.55 and −0.29

Compound	**4**·4.5MeCN	**5**·8MeCN	**6**·3MeCN	β-$L(OH)_2(Opentyl)_2$
Formula	$C_{121}H_{171.5}Zn_3N_{4.5}O_{10}$	$C_{124}H_{174}Zn_3N_8O_{10}$	$C_{128}H_{147}F_{15}Zn_6N_6O_{11}$	$C_{56}H_{79}NO_4$
Formula weight	2045.23	2132.81	2622.73	830.20
Crystal system	Triclinic	Monoclinic	Triclinic	Triclinic
Space group	$P\bar{1}$	$C2/c$	$P\bar{1}$	$P\bar{1}$
Unit cell dimensions				
a (Å)	13.71849(16)	15.8101(6)	14.8407(3)	11.5697(2)
b (Å)	17.62314(17)	22.6338(9)	18.8517(3)	17.7560(6)
c (Å)	25.3027(3)	34.2001(14)	25.1416(4)	24.6362(3)
α (°)	70.0705(10)	90	70.6500(15)	94.3452(19)
β (°)	84.4086(10)	103.2650(5)	79.6723(14)	90.0311(13)
γ (°)	81.2304(9)	90	67.7528(16)	99.536(2)
V (Å^3)	5676.87(12)	11911.7(8)	6130.9(12)	4976.3(2)
Z	2	4	2	4
Temperature (K)	100(2)	150(2)	100(2)	100(2)
Wavelength (Å)	1.54178	0.6942	0.71073	1.54178
Calculated density (g cm^{-3})	1.196	1.189	1.421	1.108
Absorption coefficient (mm^{-1})	1.19	0.62	1.24	0.52
Crystal size (mm^3)	0.20 × 0.15 × 0.10	0.20 × 0.10 × 0.08	0.06 × 0.05 × 0.04	0.16 × 0.12 × 0.08
θ (max.) (°)	70.7	27.6	26.4	68.6
Reflections measured	105 494	59 374	126 539	58 481
Unique reflections	21 180	14 789	25 065	26 581
Reflections with $I > 2\sigma(I)$	18 602	10 953	16 952	18 806
R_{int}	0.036	0.055	0.080	0.167
Number of parameters	1455	729	1536	1134
R_1 [$F^2 > 2\sigma(F^2)$]	0.075	0.048	0.052	0.127
wR_2 (all data)	0.226	0.134	0.127	0.344
GOOF, S	1.06	1.03	1.03	1.04
Largest difference peak and hole (e Å^{-3})	0.82 and −0.68	0.51 and −0.49	1.13 and −0.68	1.25 and −0.42

groups two-fold disordered, with major site occupancies of 50.0(9)%, 56.5(9)%, and 56.4(5)%, respectively. 5.5 MeCNs were accounted for with the Platon Squeeze[18] procedure which recovered 235 electrons in each of two equal voids.

For **1**·6MeCN: atoms C(41) > C(43) were modelled as split over 2 sets of positions in a *t*Bu group, with major site occupancy 72.5(16)%. In a MeCN group N(2) was modelled as split over 2 positions with major component 78.4(15)%. There is a possible, <10%, OH^- alternative to the acetate anion at O(5), but this could not be successfully modelled.

For **2**·5MeCN: the *t*Bu groups at C(7) and C(111) were modelled with Me groups split over two sets of positions

with major occupancy 83(2) and 67(3)%, respectively. The central C atom in one of the *n*-Pr groups, C(153), was similarly modelled with major component occupancy 61(3)%. The diffraction data were non-merohedrally twinned *via* a 180° rotation about [0 0 1] in both direct and reciprocal space with component ratio of 0.5095 : 0.4905(18). This problem, along with it being a very large structure resulted in the data quality being fairly poor, but the connectivity is clearly established. Several crystals were analysed, all with the same difficulties.

For **3**·4MeCN: the *t*Bu groups at C(18), C(53), and C(75) were modelled with 2-fold disorder of the methyl groups. Major site occupancies in each case were 76.9(11), 64(2), and 68(2)%, respectively. For the MeCN including N(2), the methyl group was common to both of two disorder components while the other atoms were split with major component occupancy 66(4)%. The MeCN at N(3) was modelled with all atoms split over two sets of positions with major occupancy 68(3)%. The absolute structure was reliably determined with $x = -0.001(6)$.

For **4**, the *t*Bu groups at C(7), C(72), and C(94) were modelled with 2-fold disorder of the methyl groups. The major component occupancy was 76.7(6), 62.1(10), and 76.0(11)%, respectively. Pentyl chain atoms C(48) and C(49), C(51) > C(54), and C(105) > C(108) were modelled as split over two sites with major occupancies 53.9(10), 62.8(6), and 70.3(6)%, respectively. There is a distance of around 3 Å between C(49) and C(54′) in a symmetry-related molecule, hence the disorder of the pentyl chains containing those atoms.

For **5**·8MeCN: atoms C(46) > C(49) were modelled as split over two sets of positions with major occupancy 81.9(4)%. Atoms C(52) & C(53) were modelled as split over two positions with major site occupancy 59.9(7)%.

The diffraction data for the new triclinic polymorph β-L$(OH)_2(Opentyl)_2$·MeCN were non-merohedrally twinned *via* a 180° rotation about [1 0 0] in direct space or [1 −0.25 0] in reciprocal space with component ratio of 0.5179 : 0.4821(19).

CCDC 2133113–2133121† contain the supplementary crystallographic data for this paper.

Conflicts of interest

There are no conflicts to declare.

Acknowledgements

The Chinese Scholarship Council (CSC) is thanked for the award of a PhD scholarship to Tian Xing. We thank the National Mass Spectrometry Service at Swansea, Wyatt Analytical Ltd, and the EPSRC Crystallographic Service Centre at Southampton for data. Data for **5**·8MeCN were collected at Daresbury Laboratory (Station 9.8) for which we thank the STFC for beam time. CR thanks the EPSRC for financial support in the form of a PRIF grant (EP/S025537/1).

References

1 (*a*) A.-C. Albertsson and I. K. Varma, *Biomacromolecules*, 2003, **4**, 1466–1486; (*b*) H. Tian, Z. Tang, X. Zhuang, X. Chen and X. Jing, *Prog. Polym. Sci.*, 2012, **37**, 237–280; (*c*) X. Zhang, M. Fevre, G. O. Jones and R. M. Waymouth, *Chem. Rev.*, 2018, **118**, 839–885.

2 (*a*) N. E. Kambar, W. Jeong, R. M. Waymouth, R. C. Pratt, B. G. G. Lohmeijer and J. L. Hedrick, *Chem. Rev.*, 2007, **107**, 5813–5840; (*b*) C. K. Williams and M. A. Hillmyer, *Polym. Rev.*, 2008, **48**, 1–10; (*c*) E. S. Place, J. H. George, C. K. Williams and M. H. Stevens, *Chem. Soc. Rev.*, 2009, **38**, 1139–1151; (*d*) M. Labet and W. Thielemans, *Chem. Soc. Rev.*, 2009, **38**, 3484–3504; (*e*) A. Arbaoui and C. Redshaw, *Polym. Chem.*, 2010, **1**, 801–826; (*f*) P. Lecomte and C. Jérôme, in *Synthetic Biodegradable Polymers*, Advances in Polymer Science, ed. B. Rieger, A. Künkel, G. Coates, R. Reichardt, E. Dinjus and T. Zevaco, Springer, Berlin, Heidelberg, 2011, vol. 245, pp. 173–211; (*g*) C. Redshaw, *Catalysts*, 2017, **7**, 165–178; (*h*) I. Nifant'ev and P. Ivchenko, *Molecules*, 2019, **24**, 4117; (*i*) D. M. Lynbov, A. O. Tolpygin and A. A. Trifoner, *Coord. Chem. Rev.*, 2019, **392**, 83–145; (*j*) O. Santoro, X. Zhang and C. Redshaw, *Catalysts*, 2020, **10**, 800–848; (*k*) W. Gruszka and J. A. Garden, *Nat. Commun.*, 2021, **12**, 3252.

3 (*a*) D. H. Homden and C. Redshaw, *Chem. Rev.*, 2008, **108**, 5086–5130; (*b*) M. Frediani, D. Sémeril, A. Marrioti, L. Rosi, P. Frediani, L. Rosi, D. Matt and L. Toupet, *Macromol. Rapid Commun.*, 2008, **29**, 1554–1560; (*c*) M. Frediani, D. Sémeril, D. Matt, L. Rosi, P. Frediani, F. Rizzolo and A. M. Papini, *Int. J. Polym. Sci.*, 2010, 490724; (*d*) J. D. Ryan, K. J. Gagnon, S. J. Teat and R. D. McIntosh, *Chem. Commun.*, 2016, **52**, 9071–9073; (*e*) Y. Li, K.-Q. Zhao, C. Feng, M. R. J. Elsegood, T. J. Prior, X. Sun and C. Redshaw, *Dalton Trans.*, 2014, **43**, 13612–13619; (*f*) Z. Sun, Y. Zhao, T. J. Prior, M. R. J. Elsegood, K. Wang, T. Xing and C. Redshaw, *Dalton Trans.*, 2019, **48**, 1454–1466; (*g*) O. Santoro, M. R. J. Elsegood, E. V. Bedwell, J. A. Pryce and C. Redshaw, *Dalton Trans.*, 2020, **49**, 11978–11996; (*h*) O. Santoro and C. Redshaw, *Catalysts*, 2020, **10**, 210–239; (*i*) Z. Sun, Y. Zhao, O. Santoro, M. R. J. Elsegood, E. V. Bedwell, K. Zahra, A. Walton and C. Redshaw, *Catal.: Sci. Technol.*, 2020, **10**, 1619–1639; (*j*) T. Xing, T. J. Prior, M. R. J. Elsegood, N. V. Semikolenova, I. E. Soshnikov, K. Bryliakov, K. Chen and C. Redshaw, *Catal.: Sci. Technol.*, 2021, **11**, 624–636; (*k*) S. S. Roy, S. Sarker and D. Chakraborty, *J. Inclusion Phenom. Macrocyclic Chem.*, 2021, **100**, 1–36; (*l*) O. Santoro and C. Redshaw, *Coord. Chem. Rev.*, 2021, **448**, 214173.

4 (*a*) L. H. Yao, L. Wang, J. F. Zhang, N. Tang and J. C. Wu, *J. Mol. Catal. A: Chem.*, 2012, **352**, 57–62; (*b*) M. Bouyhayi, Y. Sarazin, O. L. Casagrande and J. F. Carpentier, *Appl. Organomet. Chem.*, 2012, **26**, 681–688; (*c*) C. Y. Li, P. S. Chen, S. J. Hsu, C. H. Lin, H. Y. Huang and B. T. Ko, *J. Organomet. Chem.*, 2012, **716**, 175–181; (*d*) B. M. Chamberlain, M. Cheng, D. R. Moore, T. M. Ovitt, E. B. Lobkovsky and G. W. Coates, *J. Am. Chem. Soc.*, 2001,

123, 3229–3238; (*e*) S. Abbina and G. Du, *ACS Macro Lett.*, 2014, **3**, 689–692; (*f*) J. Bai, X. Xiao, Y. Zhang, J. Chao and X. Chen, *Dalton Trans.*, 2017, **46**, 9846–9858; (*g*) M. Köhler, P. Rinke, K. Fiederling, H. Görls, N. Ueberschaar, F. H. Schacher and R. Kretschmer, *Macromol. Chem. Phys.*, 2021, **222**, 2100187, and references therein.

5 (*a*) E. Bukhaltsev, L. Frish, Y. Cohen and A. Vigalok, *Org. Lett.*, 2005, **7**, 5123–5126; (*b*) M. J. Walton, S. J. Lancaster, J. A. Wright, M. R. J. Elsegood and C. Redshaw, *Dalton Trans.*, 2014, **43**, 18001–18009.

6 A. Bilyk, A. K. Hall, J. M. Harrowfield, M. W. Hosseini, G. Mislin, B. W. Skelton, C. Taylor and A. H. White, *Eur. J. Inorg. Chem.*, 2000, 823–826.

7 (*a*) M. V. Kniazeva, A. S. Ovsyannikov, D. R. Islamov, A. I. Samigullina, A. T. Gubaidullin, P. V. Dorovatovskii, S. E. Solovieva, I. S. Antipin and S. Ferlay, *CrystEngComm*, 2020, **22**, 7693–7703; (*b*) M. V. Kniazeva, A. S. Ovsyannikov, A. I. Samigullina, A. T. Gubaidullin, P. V. Dorovatovskii, V. A. Lazarenko, S. E. Solovieva, I. S. Antipin and S. Ferlay, *CrystEngComm*, 2022, **24**, 628–638.

8 Y. Liu, L. N. Dawe and C. M. Kozak, *Dalton Trans.*, 2019, **48**, 13699–13710.

9 D. C. Akintayo, W. A. Munzeiwa, S. B. Jonnalagadda and B. Omondi, *Inorg. Chim. Acta*, 2021, 120715.

10 D. Prochowicz, K. Sokołowski, and J. Lewiński, *Coord. Chem. Rev.*, 2014, **270–271**, 112–126.

11 A. W. Addison, T. N. Rao, J. Reedijk, J. van Rijn and G. C. Verschoor, *J. Chem. Soc., Dalton Trans.*, 1984, **7**, 1349–1356.

12 D. A. Walker, T. J. Woodman, D. L. Hughes and M. Bochmann, *Organometallics*, 2001, **20**, 3772.

13 C. Redshaw, M. R. J. Elsegood, J. A. Wright, H. Baillie-Johnson, T. Yamato, S. De Giovanni and A. Mueller, *Chem. Commun.*, 2012, **48**, 1129–1131.

14 *CrysAlis PRO, Rigaku Oxford Diffraction*, 2017–2018.

15 *SAINT and APEX 2 (2008–10) software for CCD diffractometers*, Bruker AXS Inc., Madison, USA.

16 G. M. Sheldrick, *Acta Crystallogr., Sect. A: Found. Adv.*, 2015, **A71**, 3–8.

17 G. M. Sheldrick, *Acta Crystallogr., Sect. C: Struct. Chem.*, 2015, **C71**, 3–8.

18 (*a*) P. v. d. Sluis and A. L. Spek, *Acta Crystallogr., Sect. A: Found. Crystallogr.*, 1990, **46**, 194–201; (*b*) A. L. Spek, *Acta Crystallogr., Sect. C: Struct. Chem.*, 2015, **71**, 9–18.